J. Fluid Mech. (1984), *vol.* 142, *pp.* 217–231
Printed in Great Britain

Mixing layer produced by a screen and its dependence on initial conditions

By HAKURO OGUCHI AND OSAMU INOUE
Institute of Space and Astronautical Science, Komaba 4-6-1, Meguro-ku, Tokyo 153, Japan

(Received 14 March 1983 and in revised form 28 October 1983)

This paper aims to elucidate the structure of the turbulent mixing layers, especially, its dependence on initial disturbances. The mixing layers are produced by setting a woven-wire screen perpendicular to the freestream in the test section of a wind tunnel to obstruct part of the flow. Three kinds of model geometry are treated; these model screens produced mixing layers which may be regarded as the equivalents of the plane mixing layer and of two-dimensional and axisymmetric wakes issuing into ambient streams of higher velocity. The initial disturbances are imposed by installing thin rods of various sizes along the edge of the screen or at the origin of the mixing layer. Flow features are visualized by the smoke-wire method. Statistical quantities are measured by a laser-Doppler velocimeter. In all cases large-scale transverse vortices seem to persist, although comparatively small-scale vortices are superimposed on the flow field in the mixing layer. The mixing layers are in self-preserving state at least up to third-order moments, but the self-preserving state is different in each case. The growth rates of the mixing layer are shown to depend strongly on the initial disturbance imposed.

1. Introduction

Over the past few decades, the structure of turbulent mixing layers between two uniform flows of different velocity has been studied by many investigators. There is increasing evidence that at least in some cases turbulent flows are not so random as previously considered, but have some order in their motion (Laufer 1975; Roshko 1976; Cantwell 1981). Brown & Roshko (1974) showed by flow visualization the presence of large-scale, quasi-ordered two-dimensional vortices in a fully turbulent two-dimensional mixing layer, and suggested that these quasi-ordered vortices may play an important role on the development of the shear layer. Winant & Browand (1974) presented pictures which suggest that the coalescing of neighbouring vortices is one of the primary mechanisms responsible for the development of the shear layers.

Though the mechanics and the structure of the turbulent mixing layer are thus becoming clearer, there still remain many important questions to be answered. One of them is whether the two-dimensional character of the quasi-ordered vortices persists in an environment of high turbulence level. Chandrsuda *et al.* (1978) made flow-visualization and correlation measurements for the plane mixing layer, and showed that the 'Brown–Roshko structure' becomes highly three-dimensional when the freestream turbulence level is high, or when the boundary layer on the splitter plate is turbulent. They concluded therefore that the Brown–Roshko structure is rare in practice. On the other hand, Wygnanski *et al.* (1979) studied the effects of external disturbances introduced into a mixing layer on the formation of large eddies, and showed that the two-dimensional character of the Brown–Roshko structure perseveres

in spite of strong external disturbances. They concluded, in direct contradiction to Chandrsuda *et al.*, that the Brown–Roshko structure is common in practice.

Another important issue is that there is relatively large scatter among the data given by various investigators for the growth rate of the shear layer. Weisbrot, Einav & Wygnanski (1982) obtained the growth rates of a plane turbulent mixing layer with the velocity ratio fixed, but with the actual velocities altered. The growth rates obtained varied depending on the actual velocities. The maximum growth rate was about three times larger than the minimum, for fixed velocity ratio. They attributed the variance of the growth rate to a background frequency of their facility. Batt (1975) explained that the difference between the growth rates measured for a half-jet by Liepmann & Laufer (1947) and by Wygnanski & Fiedler (1970) is mainly due to tripping or not tripping the boundary layer on the splitter plate. The growth rate in the case of a tripped boundary layer was larger than with an untripped boundary layer. Batt suggested that the initial state of the shear layer may be a significant factor in determining the growth rate of the mixing layer.

With these questions in mind, the present experiment was conducted to elucidate the structure of the turbulent mixing layers, especially its dependence on initial conditions. In most experiments, the flow is separated into two streams of different velocity by using a splitter plate (or a wall), and then fed to a test section. As suggested by Batt, however, the boundary layer growing on the splitter plate seems to provide an appreciable influence on the development of the mixing layer.

In this experiment, a mixing layer with less initial disturbance is produced by setting a screen perpendicular to the freestream in the test section of the wind tunnel. The fluid passing through the screen is decelerated, while the fluid that passes around it is accelerated. If the open-area ratio of the screen is suitably chosen, then both fluid flows may attain uniform but different velocities shortly downstream from the screen. Three kinds of model geometry are employed; a wide or narrow screen fully spanning the test section, and a disk-type screen supported by a circular ring. The mixing layers produced after these screens are regarded respectively as the equivalents of a plane mixing layer, and of the two-dimensional and axisymmetric wakes issuing into an ambient stream of higher velocity. The effect of initial disturbances on the development and structure is investigated by installing thin rods of various sizes along the edges of the screens. Qualitative features of the mixing layers are visualized by the smoke-wire method. Statistical properties of the fluctuating velocities are measured by using a laser-Doppler velocimeter (LDV).

2. Apparatus and experimental procedures

A schematic diagram of the experimental apparatus is shown in figure 1. A low-speed wind tunnel of suck-down type was used. The test section was 1500 mm long, 330 mm high and 210 mm wide, being preceded by a nozzle of contraction ratio 9:1. A honeycomb and three fine-mesh screens were installed in the nozzle. The flow in the test section can be adjusted to any speed up to 15 m/s, but in the experiment the flow speed $U_0 = 3.2$ m/s was chosen. The measured turbulence level was nearly 2%.

To realize the two streams of different velocity at the test section, a fine-mesh screen was set in the test section, perpendicular to the freestream. Three kinds of the screen geometry were tested; one is a screen 80 mm wide fully spanning the test section (case I), the second a screen of 32 mm wide also of full span (case II) and the third a disk type of screen supported by a circular ring of 50 mm in diameter (case III) (see figure 2). These screens were of 16 mesh/in. weave nylon wires 0.2 mm in diameter (the open-area ratio $\beta = 0.764$). Let us briefly describe the flow around the screens above

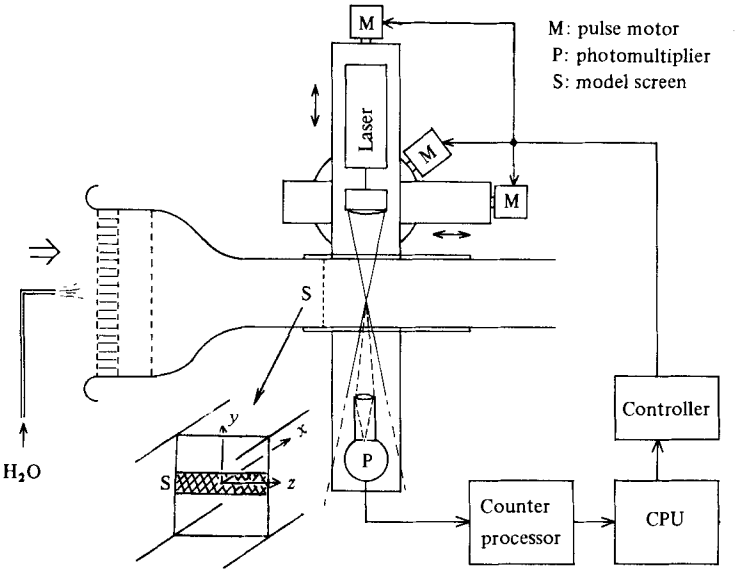

FIGURE 1. Schematic diagram of experiment.

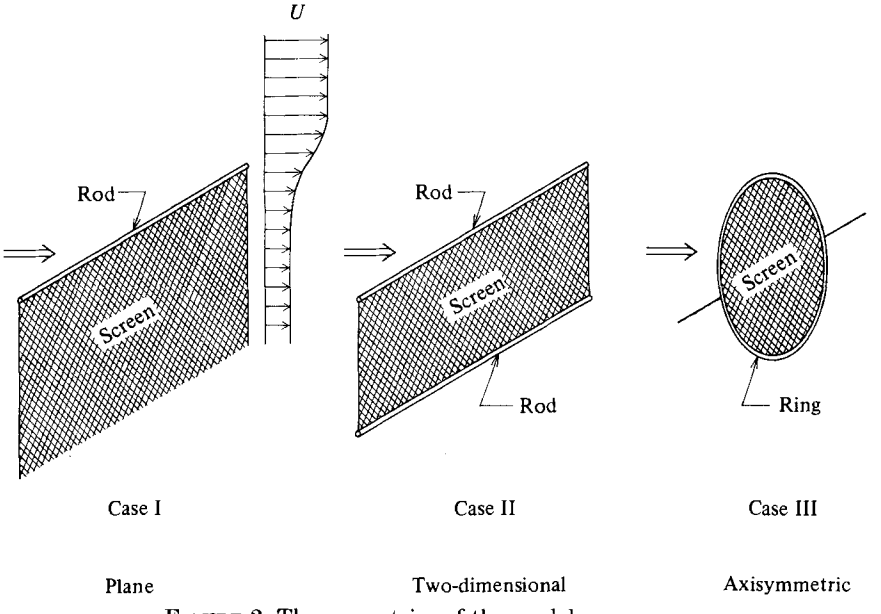

FIGURE 2. The geometries of the model screens.

mentioned. The fluid that passes through the screen is decelerated, while by continuity the flow that passes around the screen is accelerated. These two streams tend to attain their respective uniform velocities shortly downstream from the screen. This distance d, and the higher and lower stream velocities U_1, U_2, depend upon the blockage ratio of the model screen, the open area ratio of the screen, and the freestream velocity. For $U_0 = 3.2$ m/s and $\beta = 0.764$, we obtained

for case I: $U_1 = 3.63$ m/s, $U_2 = 2.50$ m/s, $d = 40$ mm;

for case II: $U_1 = 3.50$ m/s, $U_2 = 2.23$ m/s, $d = 25$ mm;

for case III: $U_1 = 3.38$ m/s, $U_2 = 2.15$ m/s, $d = 25$ mm.

It was confirmed from these measurements that, in all cases tested, the two streams

with nearly uniform different velocities are realized. This was also examined by the flow visualization shown later. Keeping this fact in mind, it can be said from the characteristic geometry of model screen that the flow of case I is the equivalent of a plane mixing layer, the flow of case II that of a two-dimensional wake issuing into the ambient stream of higher velocity, and the flow of case III that of a circular wake issuing into the ambient stream of higher velocity.

Next suppose that a suitable size of rod is installed along the edge of the screen (see figure 2). Such a rod imposes an initial disturbance on the flow in the mixing layer: the strength of the disturbance depends on the size of the rod. By installing various sizes of rod and examining the resulting flow features, we may elucidate the effect of the initial disturbance on the development and structure of the mixing layers that evolve after the screens.

The flow features were observed by means of a smoke wire method, using paraffin. This method is similar to the conventional smoke wire technique, except for the use of a smoke wire with a number of knots, which enabled us to obtain multiple, separate streaklines. The smoke wire, of 0.2 mm in diameter, was perpendicular to the freestream at 40 mm downstream from the screen. The photographs taken by flash covered a field of view in the streamwise distance x up to about 250 mm from the screen.

In addition to flow visualization, instantaneous velocities were measured with a laser-Doppler velocimeter with a 15 mW He–Ne laser. A photomultiplier detected the forward-scattered light from small seeding particles passing through the interference fringes produced by two intersective laser beams. The interval between neighbouring fringes was 3.18 μm and the angle between the two beams was 11.4°. In this experiment the seeding particles were water vapour introduced just ahead of the honeycomb from a commercial humidifier. Both laser source and detector of the LDV were mounted on the same traverse unit, which was contrived to move precisely in three orthogonal directions under computer control. The Doppler signals from the detector were fed to a counter processor (DISA 55L90) and stored on the disc of the computer.

The LDV was set such that the bisector of the two beams was normal to the freestream at the test section. The Doppler signal gives the magnitude of the velocity component along the line of intersection of the two-beam plane with the plane (x, y) normal to the bisector of the acute angle between the beams (see figure 1). If the two-beam plane is inclined at an angle θ (positive anticlockwise) to the horizontal plane, the Doppler signal gives the magnitude of the velocity component $|u\cos\theta + v\sin\theta|$, where u and v are the velocity components, in the directions x and y respectively. In this experiment for each measurement point angles of $\theta = 0°, \pm 45°$ were chosen, so that the laser signal for each angle gave respectively $|u|$, $|u+v|/\sqrt{2}$, $|u-v|/\sqrt{2}$. Since $u \gg v$ over the flow field concerned, we can regard $|u|$, $|u+v|$ and $|u-v|$ as u, $u+v$ and $u-v$ respectively. At each angle θ, 3000 instantaneous measurements were taken at each point. From the data, simple ensemble averages were evaluated by the following formulas:

$$U = \bar{u}, \quad \overline{u'^2} = \overline{(u-U)^2}, \quad \overline{u'^3} = \overline{(u-U)^3},$$

$$\overline{v'^2} = \tfrac{1}{2}[\overline{\{(u+v)-(\bar{u}+\bar{v})\}^2} + \overline{\{(u-v)-(\bar{u}-\bar{v})\}^2}] - \overline{u'^2},$$

$$\overline{u'v'} = \tfrac{1}{4}[\overline{\{(u+v)-(\bar{u}+\bar{v})\}^2} - \overline{\{(u-v)-(\bar{u}-\bar{v})\}^2}],$$

$$\overline{u'v'^2} = \tfrac{1}{6}[\overline{\{(u+v)-(\bar{u}+\bar{v})\}^3} + \overline{\{(u-v)-(\bar{u}-\bar{v})\}^3}] - \tfrac{1}{3}\overline{u'^3},$$

where primes denote the fluctuating velocity. Although the moments of u and u' can be derived up to as high an order as desired, the moments with respect to v' are limited to those shown above. For derivation of higher-order moments of v', data for more values of θ are required. Measurements were made at 18 data points across the mixing layer for $x = 25, 57, 89, 121, 153, 185$ and 217 mm downstream from the screen. Thus the maximum Reynolds number $U_1 x/\nu$ was 5×10^4.

In LDV measurements of the mixing layer in a water channel, Dimotakis & Brown (1976) reported a scatter in reproducibility as much as 5–10 % for the mean velocity U. As they noted, the 1024 samples per measurement point taken in their experiment may not be large enough. In this experiment, the scatter in reproducibility was estimated as less than 1.0 % for the mean velocity U and 1.5 % for the root mean square $(\overline{u'^2})^{\frac{1}{2}}$ of the streamwise fluctuating velocity.

3. Results and discussion

3.1. *Flow-visualization results*

Figure 3 shows photographs taken by the smoke wire method for case I at a freestream velocity $U_0 = 3.2$ m/s. A streamwise distance x up to about 250 mm is covered in the photograph. As mentioned before, the shear layer in case I is regarded as a plane mixing layer. Figure 3 (*a*) is for case I with no initial disturbance. The mixing layer is very thin and any large-scale structures do not yet grow into view. A similar flow feature was also seen for case II with no initial disturbance (see figure 4). In these cases, the large-scale structues form further downstream.

To examine the effect of the initial disturbance on the development of the mixing layer, various sizes of rod from 1–3 mm in diameter were employed. The side views of the flow are shown in figures 3 (*b–d*) for case I with various sizes of the rod. It can be seen from these figures that thicker rods (stronger initial disturbances) result in faster growth of the mixing layer, but the characteristic flow features are qualitatively similar to each other. By comparing figure 3 (*d*) with 3 (*a*) especially, the effect of the initial disturbance on the development of the mixing layer becomes evident; the large-scale structure is formed and the entrainment process is clearly seen, in which vortices engulf ambient outer streaklines and develop. The plan view of the same flow features as shown in figure 3 (*d*) is presented in 3 (*e*). For this case the smoke wire was parallel to the screen edge along the centre of the mixing layer.

There is some controversy concerning whether or not the two-dimensionality of the Brown–Roshko structure persists in an environment of higher turbulence level. Brown & Roshko (1974) and Wygnanski *et al.* (1979) suggested persistence, based on correlation measurements and visual observation, while Chandrsuda *et al.* (1978) denied it, on the basis of similar experiments. In the present experiment, the freestream turbulence level was approximately 2 % at $U_0 = 3.2$ m/s, and was much higher than those in Brown & Roshko; Chandrsuda *et al.* and Wygnanski *et al.* but lower than that in the case (iv) of Wygnanski *et al.* The maximum Reynolds number in this experiment was 5×10^4, which is the lowest of all. For cases with an initial disturbance, the plan view in figure 3 (*e*) shows comparatively small-scale disturbances over the flow field within the mixing layer. On the other hand, the side views as shown in figure 3 (*d*) shows somewhat-coherent large transverse vortices. Therefore the two-dimensionality of the structure seems to persist as a whole, so far as the region in view is concerned.

The photographs for cases II and III are presented respectively in figures 5 (*a*, *b*).

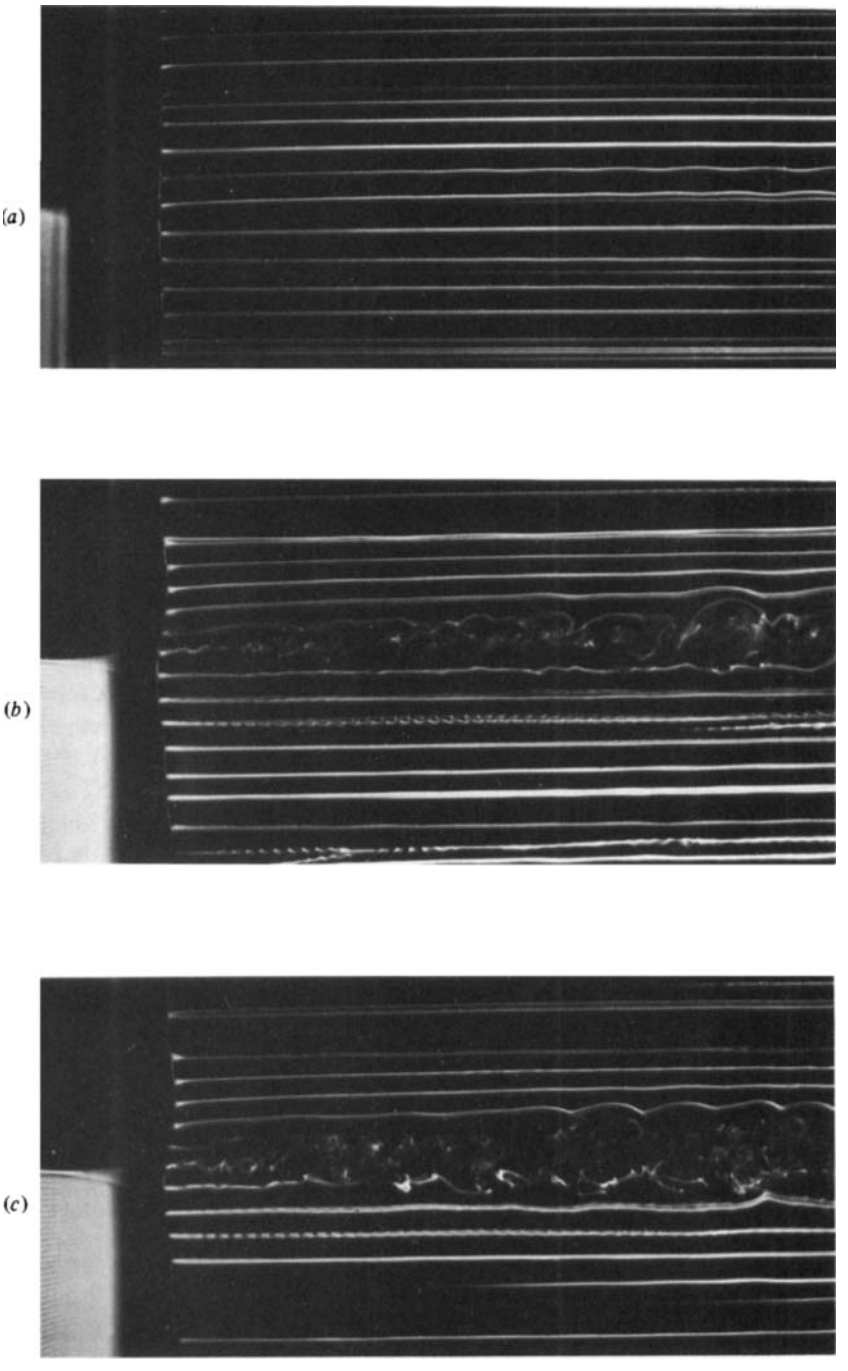

FIGURE 3. For caption see facing page.

The rods along the screen edge were 3 mm in diameter, as in figure 3(*d*). The upper and lower mixing layers do not closely interact with each other over the region covered in the photographs. It can also be seen from comparison with figure 3(*d*) for case I that the characteristic features of the mixing layers are remarkably similar in cases I, II and III, in spite of the difference in both velocity ratio $r = U_2/U_1$ and

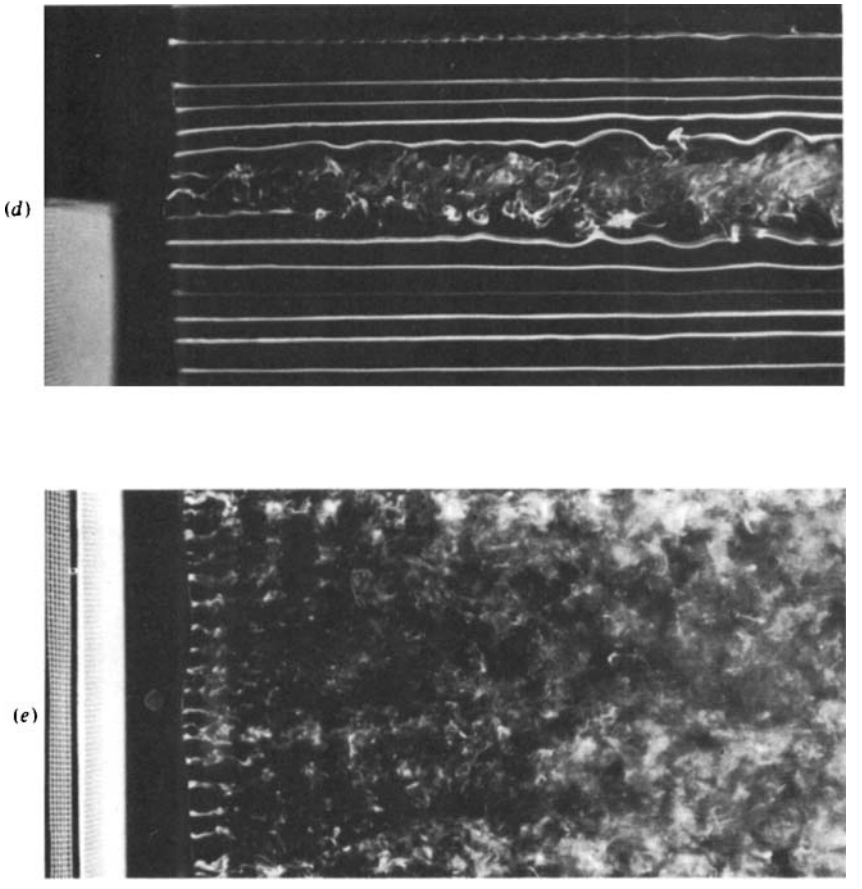

FIGURE 3. Photographs of the mixing layer for case I; $U_0 = 3.2$ m/s: (*a*) side view, without edged rod; (*b*) side view, with 1 mm edged rod; (*c*) side view, with 2 mm edged rod; (*d*) side view, with 3 mm edged rod; (*e*) plan view, with 3 mm edged rod.

type of mixing layer. These characteristic flow features can be more clearly seen from the photographs presented in figure 6, taken at a slower freestream velocity $U_0 = 1.6$ m/s. These will be confirmed quantitatively by LDV measurement described later. It should be emphasized that the vortex pattern is genuinely the one-sided 'Brown–Roshko' structure, though the disturbances shed from the rods is of Kármán vortex-street type (see figure 7).

3.2. *Results of LDV measurements*

All velocities are rendered dimensionless by the higher velocity U_1. The similarity coordinate η is defined as $\eta = (y - y_0)/x$, where the symbol y_0 denotes the y-component of a location where the mean velocity $U = \frac{1}{2}(U_1 + U_2)$.

The profiles of the mean velocity and the root mean square of the fluctuating velocity component for case I without initial disturbances are presented in the similarity form in figure 8. The mixing layer beyond $x = 150$ mm is in a self-preserving state, as shown in the figure. From these results, we can say that a relatively 'clean' mixing layer can be realized by setting a screen at the test section.

The profiles of mean products up to the third order are shown in figures 9–11 for case I, with initial disturbances produced by a 3 mm rod. It can be seen from these

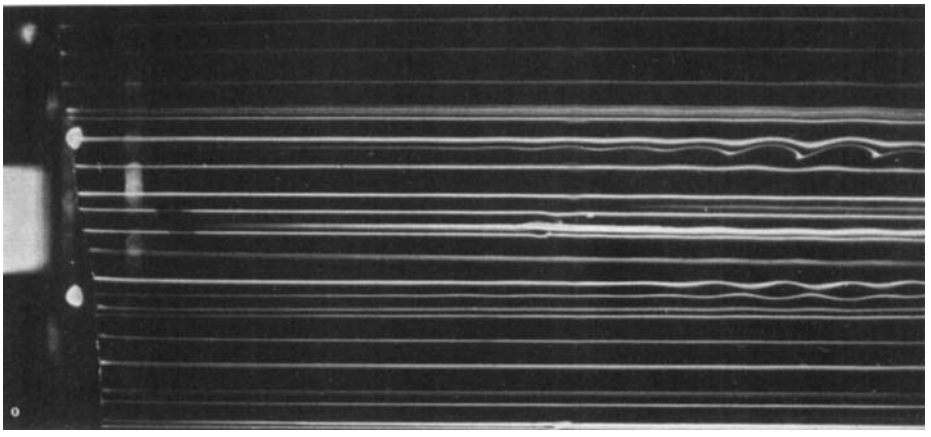

FIGURE 4. A photograph of the mixing layer for case II without edged rod; $U_0 = 3.2$ m/s.

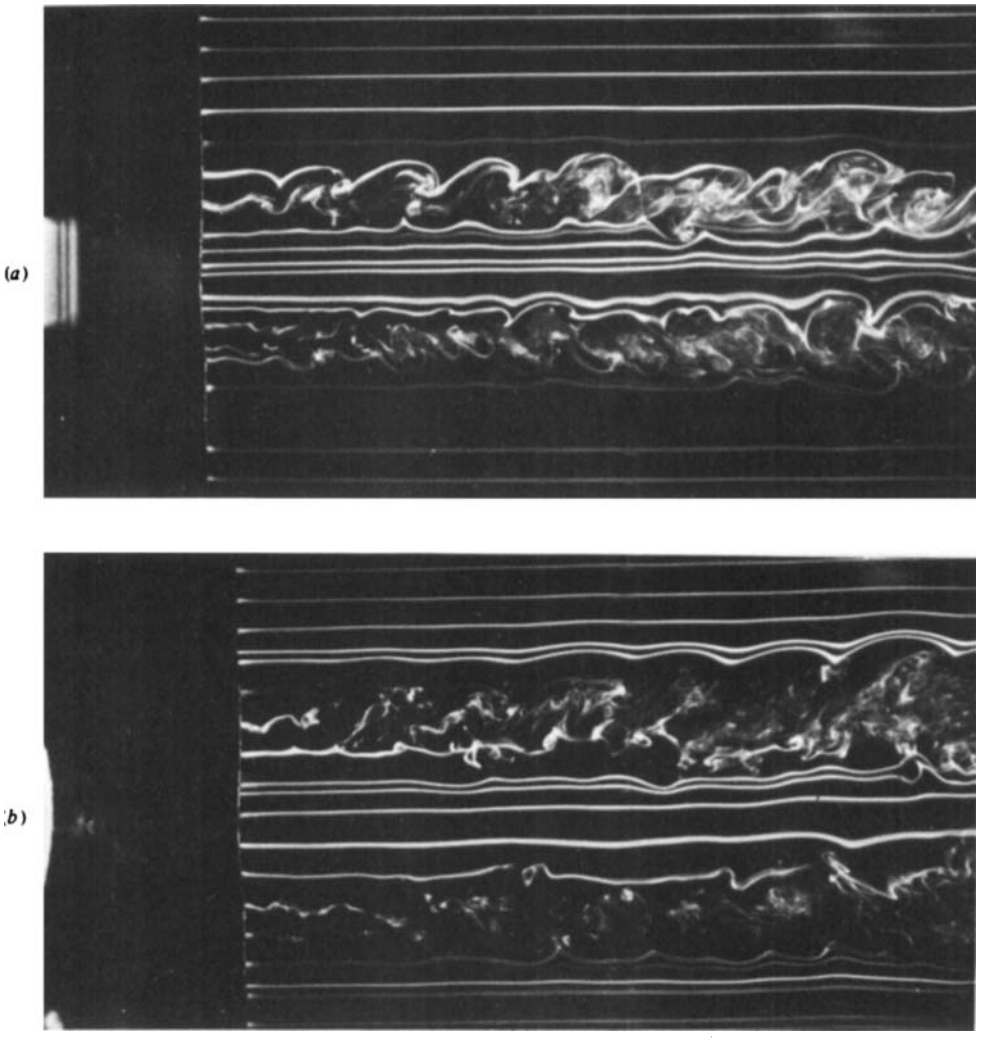

FIGURE 5. Side views of the mixing layer for cases II and III with 3 mm rod; $U_0 = 3.2$ m/s: (*a*) case II; (*b*) case III.

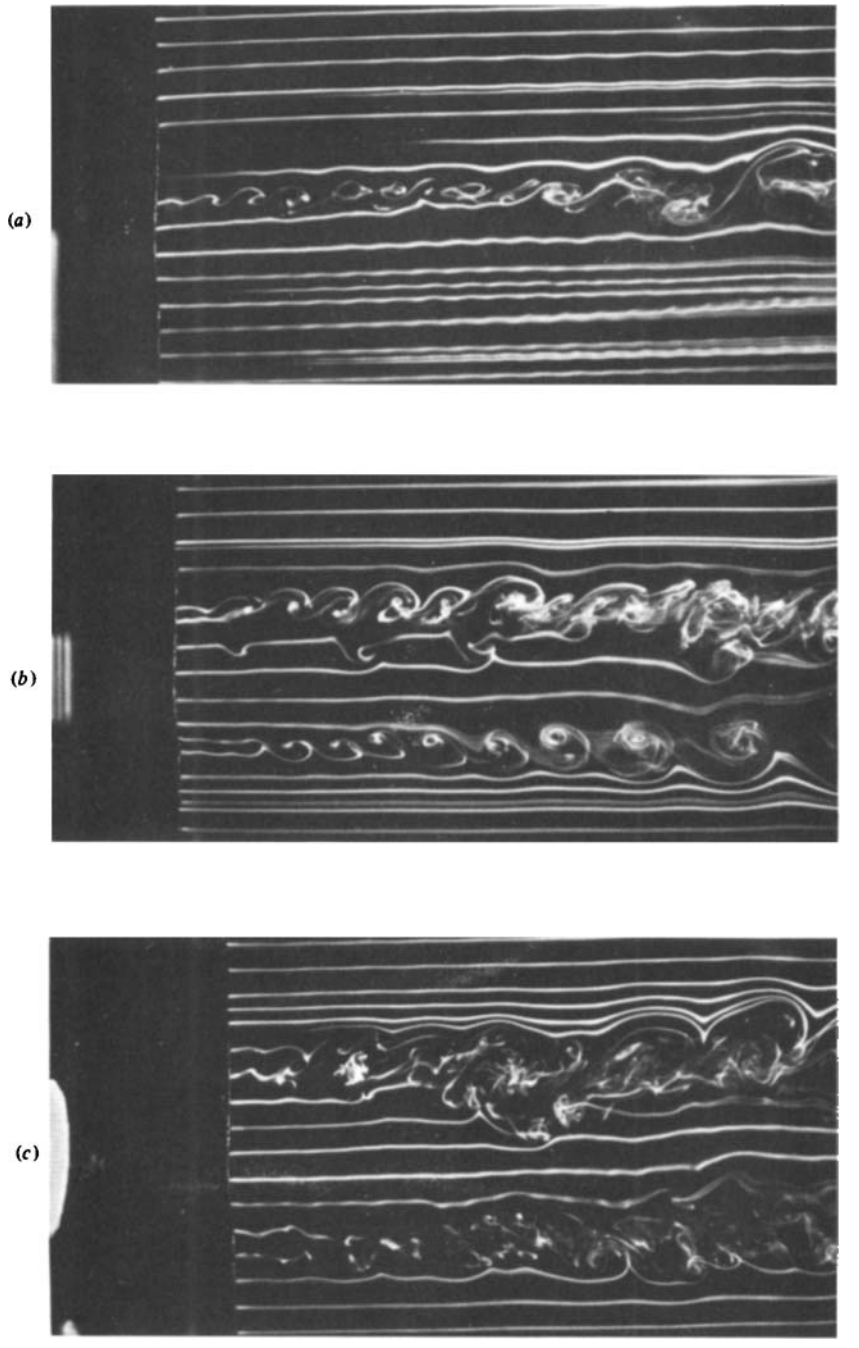

FIGURE 6. Side views of the mixing layer with lower freestream velocity; $U_0 = 1.6$ m/s, with 3 mm rod: (*a*) case I; (*b*) case II; (*c*) case III.

figures that all the statistical quantities shown are likely to be in a self-preserving state. The same can be seen from the results for cases II and III. For examples, the mean-velocity profile U and the Reynolds-stress component $-\overline{u'v'}$ for cases II and III with initial disturbances are presented in figures 12 and 13 respectively. It can be seen that the structure of the disturbed mixing layer is different from that of the undisturbed mixing layer, though both flows are in their respective self-preserving

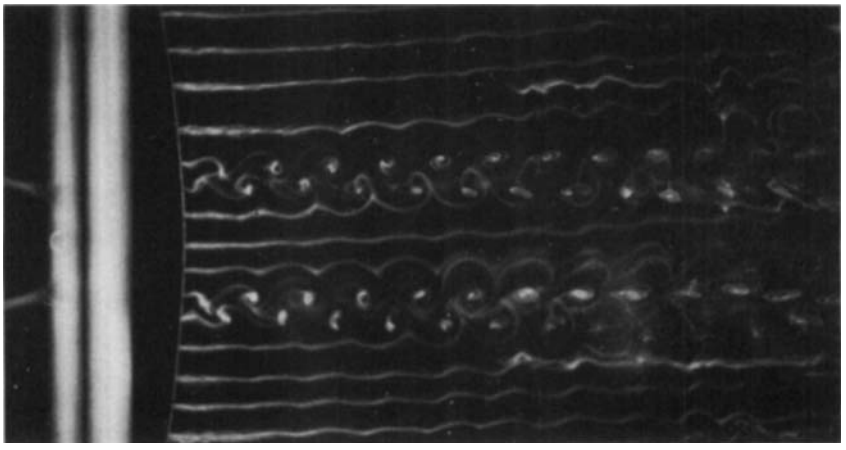

FIGURE 7. Kármán vortex street shed from the 3 mm rod for case II without screen; $U_0 = 0.8$ m/s.

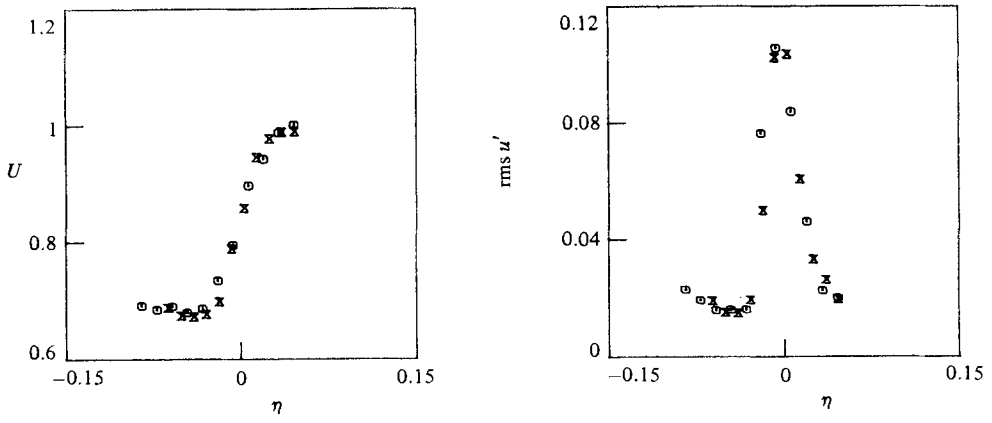

FIGURE 8. Profiles of the mean and the fluctuating velocities for case I without edged rod; $U_0 = 3.2$ m/s: ⧗, $x = 121$ mm; △, 153 mm; □, 185 mm; ◇, 217 mm.

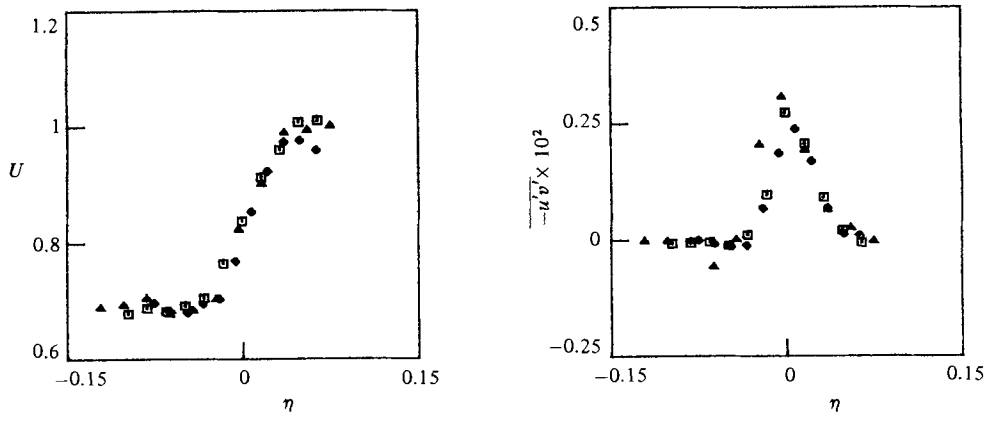

FIGURE 9. Profiles for the mean velocity and the Reynolds stress for case I with 3 mm rod (for legend see figure 8).

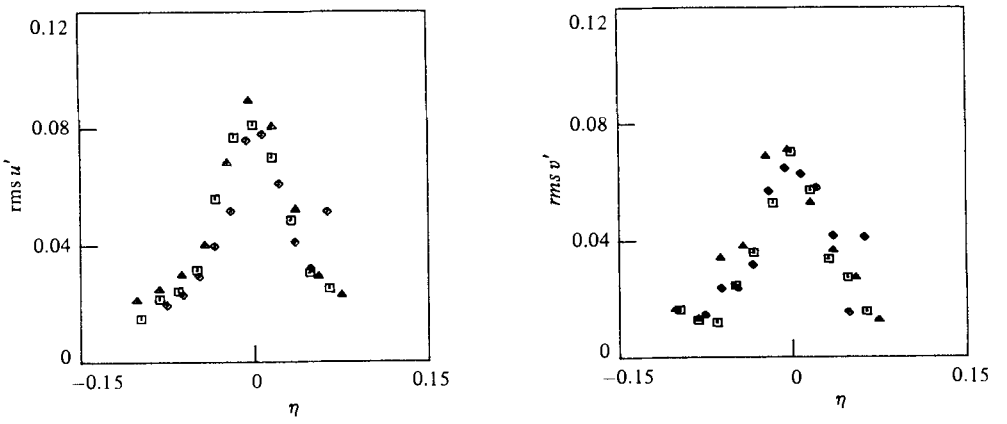

FIGURE 10. Profiles for the r.m.s. component for case I with 3 mm rod (for legend see figure 8).

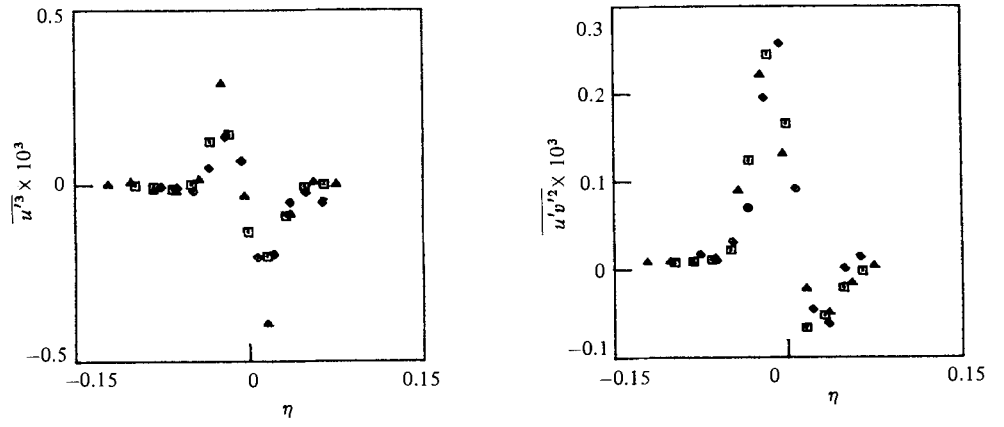

FIGURE 11. Profiles for the higher-order quantities for case I with 3 mm rod (for legend see figure 8).

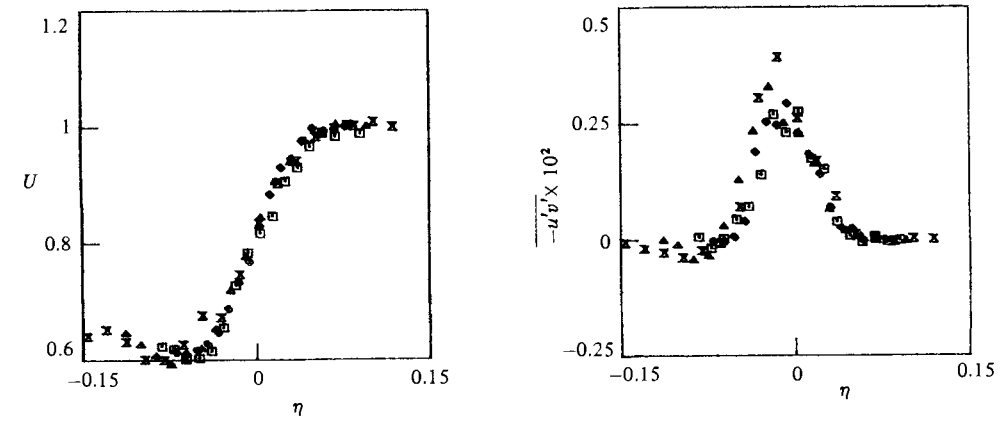

FIGURE 12. Profiles of the mean velocity and the Reynolds stress for case II with 3 mm rod.

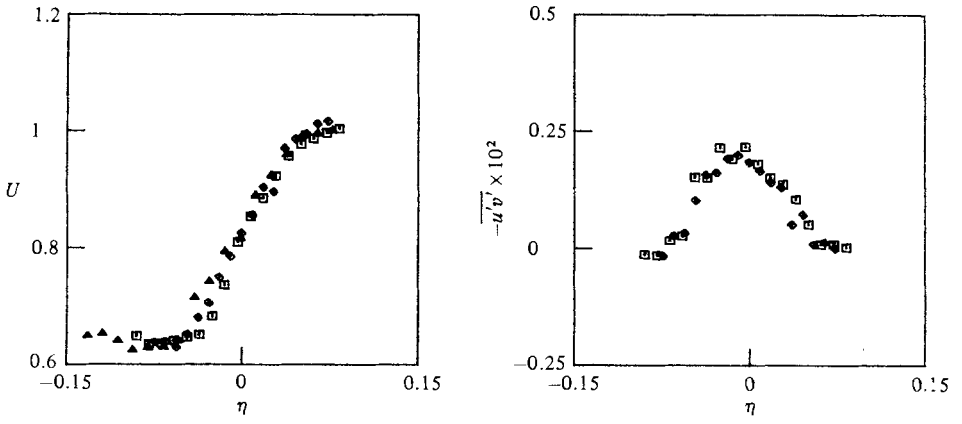

FIGURE 13. Profiles of the mean velocity and the Reynolds stress for case III with 3 mm rod.

states. This means that the memory of the initial disturbance persists in the self-preserving flows, and thus the flows are apparently not in the universal self-preserving state discussed by Townsend (1976). Champagne, Pao & Wygnanski (1976) noticed the importance of the disturbance level of the initial boundary layer along the splitter plate in determining the growth rate and turbulence intensity. They suggested that no universal self-preserving form may exist; in other words the self-preserving functions may depend on the initial conditions of the flow. Our results support this.

The relation between the growth of the mixing layer and the velocity ratio is customarily expressed as follows:

$$\frac{\delta_w}{x-x_0} = \frac{C(U_1-U_2)}{U_1+U_2} = C\lambda, \tag{1}$$

where δ_w is a representative width of a mixing layer defined by

$$\delta_w = (U_1-U_2)/(\partial U/\partial y)_{max},$$

and x_0 is a virtual origin of the mixing layer. The growth rates obtained in the present experiment are listed in table 1 and also plotted versus λ in figure 14. Brown & Roshko (1974) collected data obtained by various experiments, and gave the value of the constant C equal to 0.181 as the best fit for the data, which is shown by the solid line in figure 14. They noticed, however, that there is a relatively large scatter among the data. The present data even for the cases without initial disturbances are also scattered (see the filled symbols in figure 14).

A variety of reasons for the scattering mentioned above have been presented; for example, the effect of the state of the initial boundary layer on the splitter plate (Batt 1975; Champagne *et al.* 1976), the effect of the Reynolds number (Birch & Eggers 1973), the effect of the background frequency of the facility used (Weisbrot *et al.* 1982), and so on. The Reynolds-number effects may be considered secondary so far as the previous experiments (e.g. Weisbrot *et al.* 1982) are considered. Batt suggested, as already cited in §1, that the initial state of the mixing layer may be important in determining the growth rate. The present results also clearly show the importance of the effect of the initial state on the subsequent growth of the mixing layer; that is, in all three different geometries of the mixing layer, the larger initial disturbance leads to the larger growth rate, as can be seen from figure 14 and table 1. Figure 14

	Case	$\lambda = \frac{U_1 - U_2}{U_1 + U_2}$	$r = \frac{U_2}{U_1}$	$\frac{\delta_w}{X - X_0}$	C
I	rod 3ϕ	0.183	0.69	0.060	0.328
	no rod	0.183	0.69	0.042	0.230
II	rod 3ϕ	0.220	0.64	0.064	0.291
	no rod	0.212	0.65	0.030	0.142
III	rod 3ϕ	0.220	0.64	0.075	0.341
	rod 1ϕ	0.220	0.64	0.058	0.264
Brown & Roshko	—	—	—	—	0.181

TABLE 1. The growth rate and the velocity ratio

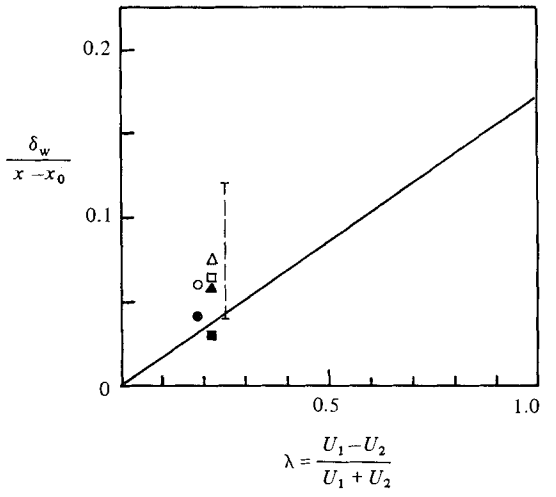

FIGURE 14. The growth rates versus the speed ratio: ○, case I (disturbed); ●, case I (undisturbed); □, case II (disturbed); ■, case II (undisturbed); △, case III (disturbed); ▲, case III (undisturbed); ——, Brown & Roshko (1974); – – – – –, Weisbrot *et al.* (1982).

also shows the results of Weisbrot *et al.* In their experiment, for a fixed value of λ ($= 0.25$), the growth rate varied with U_1 and U_2. They attributed this to the background frequency of the facility used. The background frequency, however, may not necessarily be a primary factor for the scatter of the growth rate. In fact, the present results showed different growth rates, depending on the magnitude of the initial disturbance, with the same background frequency, or at least with the same tunnel operating conditions. Recently Oster & Wygnanski (1982) experimentally studied the effect of forced periodic disturbances, introduced at the initial stage of the mixing, on the subsequent development of the mixing layer. They found that the growth of the mixing layer depends on both the amplitude and the frequency of the disturbance for fixed velocity ratio. They also found that development of the flow indicates different behaviour in three regions: the initial region (region I) in which the mixing layer grows linearly with increasing x, the resonance region (region II) in which the growth of the layer slows down or levels off, and the downstream region (region III) in which the layer again grows downstream at nearly the same growth rate as in region I. In region I the growth rate becomes larger with increase in amplitude, and the length of region I appears to be inversely proportional to the

frequency of the forced periodic disturbances. They concluded that the turbulent mixing layer depends on the initial conditions and may therefore never become a 'universal' self-preserving flow. In the present experiments, measurements were made only up to $x = 220$ mm from the model screens, and the results show qualitatively similar tendency to those in region I of Oster & Wygnanski, although the initial disturbances were imposed in a different way from theirs.

4. Concluding remarks

Relatively clean mixing layers were produced by a screen obstructing part of the test section. The structure of the mixing layer thus produced was investigated qualitatively by means of flow visualization and quantitatively by means of LDV. Special regard was paid to the effect of initial disturbances on the development of the mixing layer. The initial disturbance was imposed by a thin rod along the screen edge. Three different geometries of the mixing layer were dealt with; these may be regarded as the equivalents of the plane mixing layer, and of the two-dimensional and axisymmetric wakes issuing into an ambient stream of higher velocity.

The flow visualizations show that the two-dimensionality of the large transverse vortices appear to persist, as a whole, even in a highly turbulent flow (freestream turbulence level 2% in this experiment), though comparatively small-scale disturbances are superimposed over the flow field in the mixing layer.

It was clearly shown that the initial disturbance has a significant influence on the development of the mixing layer; in any of three different geometries of the mixing layer, larger initial disturbances lead to larger growth rate. The mixing layers dealt with in this experiment reach self-preserving states in terms of the statistical quantities at least up to the third order. However, these self-preserving flows preserved some memory of the initial conditions, so that there existed no universal self-preserving state.

The authors wish to express their sincere gratitude to Mr Shun-itsu Sato for his helpful technical assistance during this experiment.

REFERENCES

Batt, R. G. 1975 Some measurements on the effect of tripping the two-dimensional shear layer. *AIAA J.* **13**, 245–247.

Birch, S. F. & Eggers, J. E. 1973 *NASA* SP-321.

Brown, G. L. & Roshko, A. 1974 On density effects and large structures in turbulent mixing layers. *J. Fluid Mech.* **64**, 775–816.

Cantwell, B. J. 1981 Organized motion in turbulent shear flow. *Ann. Rev. Fluid Mech.* **13**, 457–515.

Champagne, F. H., Pao, Y. H. & Wygnanski, I. 1976 On the two-dimensional mixing region. *J. Fluid Mech.* **74**, 209–250.

Chandrsuda, C., Mehta, R. D., Weir, A. D. & Bradshaw, P. 1978 Effect of freestream turbulence on large structure in turbulent mixing layers, *J. Fluid Mech.* **85**, 693–704.

Dimotakis, P. E. & Brown, G. L. 1976 The mixing layer at high Reynolds number: large-structure dynamics and entrainment. *J. Fluid Mech.* **78**, 535–560.

Laufer, J. 1975 New trends in experimental turbulence research. *Ann. Rev. Fluid Mech.* **7**, 307–326.

Liepmann, H. W. & Laufer, J. 1947 Investigation of free turbulent mixing. *NACA TN* 1257.

Oster, D. & Wygnanski, I. 1982 The forced mixing layer between parallel streams. *J. Fluid Mech.* **123**, 91–130.

ROSHKO, A. 1976 Structure of turbulent shear flows: a new look. *AIAA J.* **14**, 1349–1357.

TOWNSEND, A. A. 1976 *The Structure of Turbulent Shear Flow*, 2nd edn. Cambridge University Press.

WEISBROT, I., EINAV, S. & WYGNANSKI, I. 1982 The nonunique rate of spread of the two-dimensional mixing layer. *Phys. Fluids* **25**, 1691–1693.

WINANT, D. & BROWAND, F. K. 1974 Vortex pairing: the mechanism of turbulent mixing-layer growth at moderate Reynolds number. *J. Fluid Mech.* **63**, 237–255.

WYGNANSKI, I. & FIEDLER, H. E. 1970 The two-dimensional mixing layer region. *J. Fluid Mech.* **41**, 327–361.

WYGNANSKI, I., OSTER, D., FIEDLER, H. E. & DZIOMBA, B. 1979 On the perseverance of a quasi-two-dimensional eddy-structure in a turbulent mixing layer. *J. Fluid Mech.* **93**, 325–335.